Sigma J Eng Nat Sci, Vol. 43, No. 6, pp. 1967−1981, December, 2025

Sigma Journal of Engineering and Natural Sciences
Web page info: https://sigma.yildiz.edu.tr
DOI: 10.14744/sigma.2025.1928

Research Article

Trigonometric based B-spline method for singularly perturbed sobolev problems with initial layers

Shegaye Lema CHERU[1,*], Gemechis File DURESSA[2], Tariku Birabasa MEKONNEN[1]

[1]*Department of Mathematics, Wallaga University, Nekemte, 395, Ethiopia*

[2]*Department of Mathematics, Jimma University, Jimma, 378, Ethiopia*

ARTICLE INFO

Article history
Received: 22 May 2024
Revised: 18 July 2024
Accepted: 24 September 2024

Keywords:
Pseudo-Parabolic (Sobolev) Problem; Parameter-Uniform Convergence; Singular Perturbation Problems; Trigonometric Cubic B-Spline

ABSTRACT

In this work, we investigate and numerically approximate an initial-boundary value problem governed by Sobolev type differential equation exhibiting an initial layer. The problem is approached through a finite difference framework specifically designed to remain unaffected by the presence of a small perturbation parameter, ensuring robustness and stability. A novel hybrid numerical strategy is constructed by employing a non-polynomial trigonometric cubic B-spline (TCBS) collocation technique for the spatial discretization on a uniform partition, while time advancement is carried out through an implicit Euler procedure defined over a Shishkin mesh to effectively capture sharp solution gradients. The developed scheme guarantees parameter-uniform convergence, and its theoretical stability and error properties are rigorously analyzed. A set of numerical simulations is performed to validate the effectiveness of the method, demonstrating its high accuracy, consistency, and suitability for handling singularly perturbed pseudo-parabolic problems with initial layer.

Cite this article as: Cheru SL, Duressa GF, Mekonnen TB. Trigonometric based B-spline method forsingularlyperturbedsobolevproblemswithinitiallayers.SigmaJEngNatSci2025;43(6):1967−1981.

INTRODUCTION

This section focuses on a class of singularly perturbed pseudo-parabolic equations defined in the domain $\Omega \cup [0,T]$, where $\Omega = (0,1)$ and, $Q = \Omega \times (0,T]$.

$$\begin{cases} \ell w := \varepsilon \ell_1\left[\dfrac{\partial w}{\partial t}\right] - \dfrac{\partial}{\partial x}\left[a(x,t)\dfrac{\partial w}{\partial x}\right] + b(x,t)\dfrac{\partial w}{\partial x} \\ \qquad + c(x,t)w = \aleph(x,t),\ (x,t)\in Q, \\ w(x,0) = \varphi(x), x\in\Omega, \\ w(0,t) = w(l,t) = 0, t\in(0,T], \end{cases} \tag{1}$$

where

$$\ell_1\left[\frac{\partial w}{\partial t}\right] = -\frac{\partial^3 w}{\partial t\partial x^2} + \frac{\partial w}{\partial t}.$$

Here ε denotes small perturbation parameter, while coefficient function, source term, and initial conditions are assumed to be smooth functions that fulfill specific regularity requirements, which will be detailed later.

Sobolev equations represent a distinctive category of partial differential equations (PDEs) in which the

***Corresponding author.**
*E-mail address: shegaye04@gmail.com

This paper was recommended for publication in revised form by Editor-in-Chief Ahmet Selim Dalkilic

highest-order spatial derivative is coupled with time derivative, leading to a hybrid mathematical structure that blends features of parabolic and hyperbolic equations. Such equations model a wide range of physical phenomena, thermodynamics [1], appearing in mathematical physics and fluid Dynamics [1-3], shear in second order fluids [4], astro-physics [5, 6], filtration theory [7], and propagation of long waves of small amplitude [8]. Some existence and uniqueness results of equation (1) can be found in [6,9-11]. In 1950 Sergi Sobolev started researching pseudo-parabolic equations. A significant part of the recent advances in Sobolev-type problems has been driven by the shift from classical parabolic equations to pseudo-parabolic formulations. Building upon these advancements, researchers in [11, 12] utilized advanced higher-order difference schemes to investigate delay pseudo-parabolic equations. A three-layer finite difference scheme was proposed for pseudo-parabolic equations incorporating a time-delay within the second-order derivative term [13]. Furthermore, higher-order discretization techniques were developed for one-dimensional delay pseudo-parabolic problems [14]. In addition, Zhang [15] introduced linearized compact finite difference methods to address nonlinear Sobolev-type equations involving delay terms.

The aforementioned investigations primarily address the regular (non-singular) settings. In contrast, Eq. (1) is characterized by the inclusion of mixed derivatives involving both temporal and spatial variables in its highest-order terms, an intrinsic and defining attribute of Sobolev (pseudo-parabolic) equations. Despite their significance in modeling diverse physical processes, the literature addressing problems of this type remains relatively scarce, with only a limited number of studies available [2-5,16-19], with presence of ε which makes it singularly perturbed in nature. In [5], the author examined Sobolev problems with one spatial dimension using a finite difference method (FDM) to handle boundary layers efficiently. In a related development, [17] introduced a parameter-uniform approach for initial boundary value problems (IBVPs) utilizing a standard S-mesh in the time direction. It is widely recognized that classical discretization techniques fail to maintain accuracy when the perturbation parameter takes on small values. Hence, it becomes essential to design robust and efficient numerical methods for such problems, ensuring that the accuracy of the evaluated solution remains uniform and does not deteriorate as.

The numerical estimate of singularly perturbed problems (SPPs) is inherently intricate, primarily due to the emergence of sharply localized boundary-layer phenomena within their exact solutions. The presence of small perturbation parameters causes rapid variations in narrow regions, giving rise to boundary or interior layers. As a result, conventional numerical methods often fail to capture these sharp gradients accurately and typically do not converge uniformly when the perturbation parameter becomes sufficiently small. To overcome these difficulties, specially designed parameter-robust schemes and layer-adapted meshes, such as Shishkin or Bakhvalov meshes, are widely employed to ensure stability and uniform convergence across all ranges of the perturbation parameter [20-23].

Several researchers [2-5, 16-19] have developed numerical techniques for addressing singularly perturbed Sobolev problems (SPSPs), both with and without time delays. Nonetheless, these studies have predominantly centered on approaches grounded in interpolating quadrature rules involving specific weight and basis functions. Insofar as the existing literature reveals, no further investigations have extended beyond this framework. In this study, we propose a novel computational framework that utilizes TCBS collocation technique for spatial discretization on a uniform mesh, in combination with an implicit Euler scheme functional on S-mesh for the temporal derivative.

B-spline functions have evolved into powerful and versatile analytical instruments for the numerical resolution of PDEs [19, 21-22]. Among these, TCBS collocation technique has garnered considerable scholarly interest, being effectively employed for the accurate numerical treatment of various classes of PDEs [24-26]. Unlike conventional FDM, spline-based approaches possess the inherent capability to approximate the solution with high precision at any location within the computational domain, thereby significantly enhancing spatial accuracy. Furthermore, when compared with classical polynomial B-spline formulations, the TCBS method has demonstrated superior performance, delivering more precise numerical approximations for both linear and nonlinear IBVPs. This enhanced accuracy arises from the trigonometric structure of the basis functions, which allows for better representation of oscillatory and boundary-layer behaviors often present in SPPs [25-26].

In this work, we develop a numerical method tailored for SPSPs characterized by the presence of initial layers. The key objectives are to evaluate the computational efficiency of the proposed approach, validate its accuracy, and analyze how perturbation parameters influence the formation and behavior of boundary-layer structures in the solutions. The original problem is first transformed into a more tractable formulation, after which the temporal derivative is discretized using the implicit Euler method on S-mesh. The resulting system of ordinary differential equations is subsequently solved through a TCBS collocation technique applied on a uniform spatial mesh.

PRELIMINARY FRAMEWORK AND ANALYTICAL SOLUTION

Eq. (1) is subsequently transformed into the following equivalent representation:

$$\begin{cases} \ell u := \varepsilon \dfrac{\partial w}{\partial t} - \varepsilon \dfrac{\partial^3 w}{\partial t \partial x^2} + a(x,t)\dfrac{\partial^2 w}{\partial x^2} + d(x,t)\dfrac{\partial w}{\partial x} \\ \qquad + c(x,t)w = \aleph(x,t), (x,t) \in Q, \\ w(x,0) = \varphi(x), x \in \Omega, \\ w(0,t) = w(1,t) = 0, \end{cases} \tag{2}$$

where $d(x,t) = b(x,t) - \dfrac{\partial a(x,t)}{\partial x}$ and $a(x,t)$ is a continuous functions and $\dfrac{\partial a(x,t)}{\partial x} \in C^2(\Omega)$. Eq. (2) is renowned by the presence of a mixed temporal-spatial derivative in which a small perturbation parameter ε appears in both the highest order term and the temporal derivative component, thereby delineating the specific class of SPSPs addressed in this study. The functions $(a, d, c, \aleph)(x,t)$ and $\varphi(x)$ are sufficiently smooth and satisfy the required regularity conditions, such that $a(x,t) \geq \alpha > 0$. At this stage, Eq. (2) is reformulated in an operator representation, expressed as follows:

$$\ell w = \varepsilon \frac{\partial w}{\partial t} - \varepsilon \frac{\partial^3 w}{\partial t \partial x^2} + a(x,t)\frac{\partial^2 w}{\partial x^2} + d(x,t)\frac{\partial w}{\partial x} + c(x,t)w. \tag{3}$$

The operator presented in Eq. (3) adheres to the subsequent principle of maximum.

Lemma 1. Let $\Phi(x,t) \in C^0(\overline{Q}) \cap C^2(Q)$, $\ell\Phi(x,t) \geq 0$ satisfies in $Q, \Phi(x,t) \geq 0 \text{ on } \Omega$. Then $\Phi(x,t) \geq 0, \forall (x,t) \in \overline{Q}$.

Proof. Let $(v^*, \xi^*) \in \overline{Q}$ such that $\Phi(v^*, \xi^*) = min_{(x,t)\in\overline{Q}} \Phi(x,t)$ and assume that $\Phi(v^*, \xi^*) < 0$. Now, from assumption, we have $(v^*, \xi^*) \neq \overline{Q}$ for $(v^*, \xi^*) \in Q$. As it attains minimum at (v^*, ξ^*), we have $\Phi_x = \Phi_t = \Phi_{tx} = 0$ and $\Phi_{xx} \geq 0$ at (v^*, ξ^*). Now, we have

$$\begin{aligned} \ell\Phi(x,t) &= \underbrace{\varepsilon\Phi_t(v^*, \xi^*) - \varepsilon\Phi_{txx}(v^*, \xi^*)}_{=0} - a(v^*, \xi^*)\Phi_{xx}(v^*, \xi^*) \\ &\quad + \underbrace{\tilde{b}(v^*, \xi^*)\Phi_x(v^*, \xi^*)}_{=0} + c(v^*, \xi^*)\Phi(v^*, \xi^*), \\ &= \leq a(v^*, \xi^*)\Phi_{xx}(v^*, \xi^*) + c(v^*, \xi^*)\Phi(v^*, \xi^*), \\ &< 0, \;\; \text{since } \; a(v^*, \xi^*) \geq \alpha > 0, \end{aligned}$$

which is a contradiction as $\ell\Phi(x,t) \geq 0$. Hence, $\Phi(x,t) \geq 0, \forall (x,t) \in \overline{Q}$ [19]. Lemma 2 immediately guarantees the uniqueness of the solution to the problem.

Remark 2.1. (**Friedrichs inequality**)-For a domain G with a Lipschitz boundary, there exist constants c_1, c_2 dependent on G but independent of a functions in D, such that:

$$\int_G w^2 dx \leq c_1 \sum_{k=1}^{N} \int_G \left(\frac{\partial w}{\partial x_k}\right) dx + c_2 \int_\Gamma w^2(s) ds, \tag{4}$$

holds $\forall w \in D$. For N = 1, if $D \in C^1(0, l)$, the Friedrichs inequality is expressed as follows

$$\int_0^1 w^2 dx \leq c_1 \int_0^l (w')^2 (x) dx + c_2 w^2(0),$$

$$\int_0^1 w^2 dx \leq c_1 \int_0^l (w')^2 (x) dx + c_2 w^2(l),$$

$$\int_0^1 w^2 dx \leq c_1 \int_0^l (w')^2 (x) dx + c_2 \left[w^2(0) + w^2(l)\right].$$

If a function in D satisfy additional conditions, such that $w(0) = 0$ or $w(l) = 0$, special cases of the previously derived estimates are obtained. Specifically, if $D_1 \subseteq D$ with $w(0) = 0 = w(l)$, the estimates takes the form:

$$\int_0^l w^2 dx \leq c_1 \int_0^l (w')^2 (x) dx, \quad w \in D_1. \tag{5}$$

By selecting one of the estimates for c_1, we derive the following inequality:

$$\int_0^1 w^2 dx \leq c_1 \frac{(l-0)}{\pi^2} \int_0^l (w')^2 (x) dx, \tag{6}$$

which is valid for for all $w \in D_1$, that is for all $w \in D$ which satisfies the above condition.

Remark 2.2. At the critical points (0,0) and (l,0), the functions $\varphi(x)$ and $\aleph(x,t)$ gratify the subsequent compatibility requirements:

$$\varphi(0) = \varphi(l) = 0 \tag{7}$$

and

$$\begin{cases} -\dfrac{\partial}{\partial x}\left(a(0,0)\dfrac{d\varphi(0)}{dx}\right) + b(0,0)\dfrac{d\varphi(0)}{dx} + c\varphi(0) = \aleph(0,0), \\ -\dfrac{\partial}{\partial x}\left(a(l,0)\dfrac{d\varphi(l)}{dx}\right) + b(l,0)\dfrac{d\varphi(l)}{dx} + c\varphi(l) = \aleph(l,0). \end{cases} \tag{8}$$

Lemma 2. Let $\dfrac{\partial a}{\partial x}, \dfrac{\partial b}{\partial x}, c, \aleph \in C^2(\overline{\Omega})$ and

$$\alpha + \pi^{-2} l^2 \zeta_0 > 0, \text{ where } \zeta_0 = \min_{\overline{Q}} \left(c - \frac{1}{2}\frac{\partial b}{\partial x}\right). \tag{9}$$

Accordingly, the solution of Eq. (1) satisfies the ensuing estimations as established in [13, 16-17].

$$\left|\frac{\partial^{k+z} w}{\partial t^k \partial x^z}\right| \le C\varepsilon^{-k},\ (x,t)\in\overline{Q}, \quad k=0,1;\ \ z=0,1,2. \quad (10)$$

Proof. Multiply both sides of Eq. (1) by $w(x,t)$. In this case, we obtain

$$\left(\ell w, w\right)_0 = \left(\aleph, w\right)_0. \quad (11)$$

Expanding Eq. (11) through the inner product yields:

$$\left(-\varepsilon\frac{\partial^3 w}{\partial t \partial x^2}, w\right)_0 + \left(\varepsilon\frac{\partial w}{\partial t}, w\right)_0 - \left(\frac{\partial}{\partial x}\left(a\frac{\partial w}{\partial t}\right), w\right)_0 + \left(b\frac{\partial w}{\partial x}, w\right)_0 + \left(cw, w\right)_0 = \left(\aleph, w\right)_0.$$

We now employ the technique of energy-based inequalities, achieved by performing a scalar multiplication with $w(x,t)$ wherein

$\left(w,v\right)=\int_0^l wv dx,\ \ \|w\|_0^2 = \left(w,w\right)_0$. Here

$$\left(-\varepsilon\frac{\partial^3 w}{\partial t\partial x^2}, w\right)_0 = -\varepsilon\int_0^l \frac{\partial^3 w}{\partial t \partial x^2} w dx = \frac{\varepsilon}{2}\frac{\partial}{\partial t}\left\|\frac{\partial w}{\partial x}\right\|_0^2,$$

$$\left(\varepsilon\frac{\partial w}{\partial t}, w\right)_0 = \int_0^l \varepsilon\frac{\partial w}{\partial t} w dx = \frac{1}{2}\int_0^l \left(w^2\right)_t dx = \frac{\varepsilon}{2}\frac{\partial}{\partial t}\int_0^l w^2 dx = \frac{\varepsilon}{2}\frac{\partial}{\partial t}\|w\|_0^2,$$

$$\left(\left(aw_x\right)_x, w\right)_0 = \int_0^l \left(aw_x\right)_x w dx = \left[aw_x w\right]_0^l - \alpha\int_0^l w_x^2 dx = -\alpha\left\|\frac{\partial w}{\partial x}\right\|_0^2,$$

since $a(x,t) \ge \alpha > 0$,

$$\left(bw_x, w\right)_0 = \int_0^l bw_x w dx = \int_0^l b\left(w^2\right)_x dx = \left(w^2 b\right)_0^l - \frac{1}{2}\frac{\partial b}{\partial x}\int_0^l w^2 dx = -\frac{1}{2}\frac{\partial b}{\partial x}\|w\|_0^2,$$

$$\left(cw, w\right)_0 = \int_0^l cw^2 dx = c\|w\|_0^2, \ \text{ since } c\in C^2\left(\overline{\Omega}\right),$$

$$\left|\left(\aleph, w\right)\right| \le \|w\|_0 \|\aleph\|_0 .$$

Upon inserting this expression into Eq. (1) and performing subsequent algebraic manipulations, we obtain:

$$\frac{\varepsilon}{2}\frac{d}{dt}\left(\left\|\frac{\partial w}{\partial x}\right\|_0^2 + \|w\|_0^2\right) \le -\alpha\left\|\frac{\partial w}{\partial x}\right\|_0^2 + \frac{1}{2}\frac{\partial b}{\partial x}\|w\|_0^2 - c\|w\|_0^2 + \|w\|_0\|\aleph\|_0,$$

$$\begin{aligned}\varepsilon\frac{d}{dt}\left(\left\|\frac{\partial w}{\partial x}\right\|_0^2 + \|w\|_0^2\right) &\le -2\alpha\left\|\frac{\partial w}{\partial x}\right\|_0^2 + \frac{\partial b}{\partial x}\|w\|_0^2 - 2c\|w\|_0^2 + 2\|w\|_0\|\aleph\|_0,\\ &\le -2\alpha\left\|\frac{\partial w}{\partial x}\right\|_0^2 - 2\left(c - \frac{1}{2}\frac{\partial b}{\partial x}\right)\|w\|_0^2 + 2\|w\|_0\|\aleph\|_0,\\ &\le -2\alpha\left\|\frac{\partial w}{\partial x}\right\|_0^2 - 2\zeta_0\|w\|_0^2 + 2\|w\|_0\|\aleph\|_0,\\ &= -2\alpha\left\|\frac{\partial w}{\partial x}\right\|_0^2 - 2\zeta_0\|w\|_0^2 + \Re(t),\end{aligned}$$

where $\Re(t) = 2\|w\|_0\|\aleph\|_0$. Now, we have two cases:

1. If $\alpha \le \zeta_0$, then

$$\varepsilon\chi'(t) \le -2\alpha\chi(t) + \Re(t), \quad (12)$$

where $\chi(t) = \left\|\frac{\partial w}{\partial x}\right\|_0^2 + \|w\|_0^2.$

2. Given $\alpha \le \zeta_0$, and $0 < \vartheta < 1$, employing the embedding inequality in Eq. (6) leads to the following result:

$$\begin{aligned}\alpha\left\|\frac{\partial w}{\partial x}\right\|_0^2 + \zeta_0\|w\|_0^2 &= \alpha\left(1-\vartheta\right)\left\|\frac{\partial w}{\partial x}\right\|_0^2 + \alpha\vartheta\left\|\frac{\partial w}{\partial x}\right\|_0^2 + \zeta_0\|w\|_0^2,\\ &\ge \alpha\left(1-\vartheta\right)\left\|\frac{\partial w}{\partial x}\right\|_0^2 + \left(\alpha\vartheta\frac{\pi^2}{l^2} + \zeta_0\right)\|w\|_0^2,\end{aligned}$$

choosing ϑ from equality $\alpha\left(1-\vartheta\right) = \alpha\vartheta\frac{\pi^2}{l^2}$ and considering Eq. (9), we obtain

$$\vartheta = \frac{1-\alpha^{-1}\zeta_0}{1+\pi^2 l^{-2}};\ \ 1-\vartheta = \frac{\pi^2 l^{-2} + \alpha^{-1}\zeta_0}{1+\pi^2 l^{-2}}.$$

By inserting these expressions into the preceding equation, we arrive at:

$$\varepsilon\chi'(t) \le -2\frac{\alpha\pi^2 l^{-2} + \zeta_0}{1+\pi^2 l^{-2}}\chi(t) + \Re(t). \quad (13)$$

Hence, combining the results of Eqs. (12) and (13) yields:

$$\varepsilon\chi'(t) \le -2c_0\chi(t) + \Re(t),$$

$$\text{where } c_0 = \begin{cases} \alpha & \text{if } \alpha \le \zeta_0 \text{ for case 1,} \\ \dfrac{\alpha\pi^2 l^{-2} + \zeta_0}{1+\pi^2 l^{-2}} & \text{if } \alpha > \zeta_0 \text{ for case 2.}\end{cases} \quad (14)$$

Furthermore, for $\Re(t)$ expression, by using $\left|\left(w,v\right)\right| \le \mu\|w\|^2 + \frac{1}{4\mu}\|v\|^2$ inequality, we obtain

$$2\|w\|_0\|\aleph\|_0 \le 2c_0\|w\|_0^2 + \frac{1}{2c_0}\|\aleph\|_0^2 \Rightarrow 2\|w\|_0\|\aleph\|_0 \le c_0\|w\|_0^2 + \frac{1}{c_0}\|\aleph\|_0^2,$$

where $c_0 = 2c_0$ is a constant. Now, substituting this values in place of $\Re(t)$, we have

$$\varepsilon\chi'(t) \le -2c_0\chi(t) + c_0\|w\|_0^2 + \frac{1}{c_0}\|\aleph\|_0^2 \le -c_0\chi(t) + c_0^{-1}\|\aleph\|_0^2.$$

Since $-c_0\left\|\frac{\partial w}{\partial x}\right\|_0^2$ is a constant and omitting from the expression, we get

$$\varepsilon\chi'(t) \le -c_0\chi(t) + c_0^{-1}\|\aleph\|_0^2. \tag{15}$$

From Eq. (15) and Gronwalls's inequality, the integrating factor is $I.F = e^{\int(p(x))dx}$, where $p(x)$ depends on x. After some manipulation, we obtain:

$$\frac{d\chi(t)}{dt}e^{\frac{c_0}{\varepsilon}t} \le -\frac{c_0}{\varepsilon}\chi(t)e^{\frac{c_0}{\varepsilon}t} + \frac{c_0^{-1}}{\varepsilon}\|\aleph\|_0^2 e^{\frac{c_0}{\varepsilon}t}, \text{ multiply by I.F}$$

$$\Rightarrow \frac{d}{dt}\left(\chi(t)e^{\frac{c_0}{\varepsilon}t}\right) \le \frac{c_0^{-1}}{\varepsilon}\|\aleph\|_0^2 e^{\frac{c_0}{\varepsilon}t},$$

integrating both sides with respect to t

$$\Rightarrow \chi(t)e^{\frac{c_0}{\varepsilon}t} \le \frac{c_0^{-1}}{\varepsilon}\int_0^t \|\aleph(\tau)\|_0^2 e^{-\frac{c_0}{\varepsilon}(t-\tau)}d\tau + \chi(0),$$

$$\Rightarrow \chi(t) = \chi_0 e^{-\frac{c_0}{\varepsilon}t} + c_0^{-2}\max_{0\le\tau\le t}\|\aleph(\tau)\|_0^2\left(1-e^{-\frac{c_0 t}{\varepsilon}}\right),$$

where $\chi_0 = \|\varphi\|_1^2$

Thus, from the above, we get

$$\left\|\frac{\partial w}{\partial x}\right\|_0^2 + \|w\|_0^2 \le \chi_0 e^{-\frac{c_0 t}{\varepsilon}} + c_0^{-2}\max_{0\le\tau\le t}\|\aleph(\tau)\|_0^2,$$

$$\text{since } \max\left(1-e^{-\frac{c_0 t}{\varepsilon}}\right) = 1.$$

Next, by embedding inequality and Poincare inequality, $\frac{l}{4}\left\|\frac{\partial w}{\partial x}\right\|_0^2 \ge \left\|\frac{\partial w}{\partial x}\right\|_{\infty,\Omega}^2$, we get

$$\|w\|_{\infty,\Omega}^2 \le \frac{l}{4}\chi_0 e^{-\frac{c_0 t}{\varepsilon}} + \frac{l}{4}c_0^{-2}\max_{0\le\tau\le t}\|\aleph(\tau)\|_0^2 \Rightarrow |w(x,t)|$$
$$\le \frac{\sqrt{l}}{2}\left(\chi_0^{1/2}e^{-\frac{c_0 t}{\varepsilon}} + c_0^{-1}\max_{0\le\tau\le t}\|\aleph(\tau)\|_0\right),$$

which proves Eq. (10) for $z = k = 0$. Again multiply Eq. (1) by $\frac{\partial^2 w}{\partial x^2}$, we obtain

$$\varepsilon\left(\frac{\partial w}{\partial t}, \frac{\partial^2 w}{\partial x^2}\right)_0 - \varepsilon\left(\frac{\partial^3 w}{\partial t\partial x^2}, \frac{\partial^2 w}{\partial x^2}\right)_0 - \left(\frac{\partial}{\partial x}\left(a\frac{\partial w}{\partial x}\right), \frac{\partial^2 w}{\partial x^2}\right)_0$$
$$+\left(b\frac{\partial w}{\partial x}, \frac{\partial^2 w}{\partial x^2}\right)_0 + \left(cw, \frac{\partial^2 w}{\partial x^2}\right)_0 = \left(\aleph, \frac{\partial^2 w}{\partial x^2}\right)_0 \Rightarrow \left(\ell u, \frac{\partial^2 w}{\partial x^2}\right)_0$$
$$= \left(\aleph, \frac{\partial^2 w}{\partial x^2}\right)_0.$$

Analogous to the earlier scenarios, following appropriate algebraic manipulations and reorganization, we obtain:

$$\left\|\frac{\partial^2 w}{\partial x^2}\right\|_0^2 \le C, \tag{16}$$

Given that $\varphi'' \in L_2(\Omega)$ and by using the boundedness of $\|w\|_0$ and $\left\|\frac{\partial w}{\partial x}\right\|_0$. The estimate Eq. (16), in turn $\left\|\frac{\partial w}{\partial x}\right\|_{\infty,\Omega} \le C\left\|\frac{\partial^2 w}{\partial x^2}\right\|_0$ gives Eq. (10) for $k = 0, z = 1$. Once more, by utilizing the given identity, $\left(\ell w, \frac{\partial^3 w}{\partial x^2\partial t}\right)_0 = \left(\aleph, \frac{\partial^3 w}{\partial x^2\partial t}\right)_0$, we obtain

$$\left\|\frac{\partial^3 w}{\partial t\partial x^2}\right\|_0^2 + \left\|\frac{\partial^2 w}{\partial t\partial x^2}\right\|_0^2 \le \frac{C}{\varepsilon^2}\left(\|w\|_0^2 + \left\|\frac{\partial w}{\partial x}\right\|_0^2 + \left\|\frac{\partial^2 w}{\partial x^2}\right\|_0^2 + \|\aleph\|_0^2\right),$$

which leads to Eq. (10) for $k = 1, z = 0,1$ by using just proved estimates for $\left\|\frac{\partial^z w}{\partial x^z}\right\|_0^2, (z = 0,1,2)$.

In conclusion, expressing Eq. (1) in the following form yields:

$$\varepsilon\frac{\partial^3 w}{\partial x^2\partial t} + a(x,t)\frac{\partial^2 w}{\partial x^2} = \Gamma(x,t),$$

with

$$\Gamma(x,t) = \varepsilon\frac{\partial w}{\partial t} - \frac{\partial a}{\partial x}\frac{\partial w}{\partial x} + b\frac{\partial w}{\partial x} + cw - \aleph, \text{ and } |\Gamma(x,t)| \le C,$$

The estimates Eq. (10) then follows immediately for $k = 0,1$, $z = 2$.

Lemma 3. Assume $\frac{\partial a}{\partial t}, \frac{\partial^2 a}{\partial t\partial x}, \frac{\partial b}{\partial t}, \frac{\partial c}{\partial t}, \frac{\partial\aleph}{\partial t} \in C(\overline{\Omega})$ and assumptions of Lemma 2 are valid. Then the estimate:

$$\left\|\frac{\partial^{l+z} w}{\partial t\partial x^z}\right\| \le C\left\{1 + \frac{1}{\varepsilon}e^{-\frac{\alpha_0 t}{\varepsilon}}\right\}, \; t\in[0,T], \; z = 0,1,2, \tag{17}$$

holds where $\alpha_0 = c_0/2$ and c_0 is given by Eq. (14).

Proof. The argument is presented in [16-17, 19].

NUMERICAL METHOD IMPLEMENTATION

Mesh Generation and Discretization

The domain Q is partitioned using mesh points $\Lambda = \Lambda_N \times \Lambda_M$, where $\Lambda_N = \{x_i = ih{:}i = 1(1)N - 1, h = l/N\}$ and $\Lambda_M = \{0 = t_1 < t_2 < \cdots < t_M = T, \tau_j = t_j - t_{j-1}\}$. The temporal mesh Λ_M is chosen as a piecewise-uniform grid. A fitted piecewise-uniform S-mesh is introduced on $[0,T]$ to resolve the initial layer at $t = 0$. The interval is split into $[0,\sigma]$ and $[\sigma,T]$, each divided into $M/2$ equal parts, with the transition point σ defined as in .

$$\sigma = min\left\{\frac{T}{2}, \alpha_0^{-1}\varepsilon \ln(M)\right\}, \quad (18)$$

where α_0 is constant, $\alpha_0 = c_0/2$ and c_0 is given in Eq. (14). Since $\sigma \ll T$, the mesh is refined over $[0,\sigma]$ and coarser over $[\sigma,T]$. Let τ_1 and τ_2 denote the step sizes these respective subintervals. Now, $\tau_1 = 2\sigma M^{-1}$, $\tau_2 = 2(T-\sigma)M^{-1}$, $\tau_1 \le TM^{-1}, TM^{-1} \le \tau_2 < 2TM^{-1}, \tau_2 + \tau_2 = 2TM^{-1}$, so we get

$$\overline{\Lambda}_M = t_j = \begin{cases} j\tau_1, & \text{if } \ j = 0(1)M/2, \\ \sigma + (j - M/2)\tau_2, & \text{if } \ j = M/2(1)M. \end{cases} \quad (19)$$

It is assumed that $\sigma = \alpha_0^{-1}\varepsilon\ln(M)$; otherwise N grows exponentially relative to ε.

Semi-Discretization in Time

The time domain is discretized on an S-mesh with step size τ_j, while x is kept continuous, yielding the following ODE system.

$$\begin{aligned} &-\left(\varepsilon + \tau_j a^{j+1}(x)\right)\left(w_{xx}(x)\right)^{j+1} + d^{j+1}(x)\left(w_x(x)\right)^{j+1} \\ &+\left(\varepsilon + \tau_j c^{j+1}(x)\right)w^{j+1}(x) \\ &+\varepsilon\left(w_{xx}(x)\right)^j - \varepsilon w^j(x) = g(x,t_{j+1}), \\ &w(x,0) = w^0(x) = \varphi(x),\ x\in\overline{\Omega}, \\ &w^{j+1}(0) = w^{j+1}(l) = 0,\ 0 \le j \le M,\ t\in(0,T], \end{aligned} \quad (20)$$

At the $(j + 1)th$ time step, Eq. (20) takes the form:

$$\begin{cases} \ell_\varepsilon^M w^{j+1}(x) = -\left(\varepsilon + \tau_j a^{j+1}(x)\right)\left(w_{xx}(x)\right)^{j+1} + d^{j+1}(x)\left(w_x(x)\right)^{j+1} \\ \qquad +\left(\varepsilon + \tau_j c^{j+1}(x)\right)w^{j+1}(x) = g(x,t_{j+1}), \\ \qquad w(x,0) = w^0(x) = \varphi(x),\ x\in\overline{\Omega}, \\ \qquad w^{j+1}(0) = w^{j+1}(l) = 0,\ 0 \le j \le M,\ t\in(0,T], \end{cases} \quad (21)$$

where, $g(x,t_{j+1}) = -\varepsilon\left(w_{xx}(x)\right)^j + \varepsilon w^j(x) + \tau_j \aleph^{j+1}(x)$.

Lemma 3.1. (Semi-Discrete Version of Maximum Principle.) Let $\Phi^{j+1}(x)$ be sufficiently smooth on $\overline{\Lambda}$. If $\Phi^{j+1}(0) \ge 0$, $\Phi^{j+1}(1) \ge 0$ and $\ell_\varepsilon^M \Phi^{j+1}(x) \ge 0, x\in\Lambda$, then $\Phi^{j+1}(x) \ge 0,\ \forall x\in\overline{\Lambda}$.

Proof. Let σ^* is such that $\Phi_{j+1}(\sigma^*) = \min_{x\in\overline{\Omega}} \Phi_{j+1}(0) < 0$. We know that $\sigma^* \notin \{0,1\} \Rightarrow \sigma^* \in (0,1)$. Using extrema values, $\frac{d}{dx}\Phi_{j+1}(\sigma^*) = 0$ and $\frac{d^2\Phi_{j+1}(\sigma^*)}{dx^2} \ge 0$. Then we have

$$\begin{aligned} \ell_\varepsilon^M \Phi^{j+1}(\sigma^*) &= -\left(\varepsilon + \tau_j a^{j+1}(\sigma^*)\right)\left(\Phi_{xx}\right)^{j+1}(\sigma^*) \\ &\quad + d^{j+1}(\sigma^*)\left(\Phi_x\right)^{j+1}(\sigma^*) \\ &\quad +\left(\varepsilon + \tau_j c^{j+1}(\sigma^*)\right)\Phi^{j+1}(\sigma^*), \\ &\le \left(\varepsilon + \tau_j c^{j+1}(\sigma^*)\right)\Phi^{j+1}(\sigma^*), \\ &\le 0,\ as\ \left(\varepsilon + \tau_j c^{j+1}(x)\right) > 0, \end{aligned}$$

given that $\ell_\varepsilon^M \Phi^{j+1}(\sigma^*) < 0$ which is a contradiction to $\ell_\varepsilon^M \Phi^{j+1}(\sigma^*) \ge 0,\ \forall x\in\overline{\Omega}$. Therefore, $\Phi^{j+1}(x) \ge 0, \forall x\in\overline{\Omega}$. Thus, ℓ_ε^M satisfies the semi-discretized form of the maximum principle.

Time Semi-Discretization: Error Analysis

Let $w^{j+1}(x)$ reprent the semi-discrete approximation of the exact solution $w(x,t_{j+1})$ of Eq. (4) at time level τ_j. Then, applying the implict Euler method, the semi-discrete scheme for Eq. (2.1) can be expressed as:

$$\begin{cases} \Upsilon^0(x) = \varphi_0(x),\ x\in\overline{\Omega}, \\ \ell_\in^M \Upsilon^{j+1}(x) = g(x,t_{j+1}), \\ \Upsilon^{j+1}(0) = 0 = \Upsilon^{j+1}(l), 0 \le j \le M, t\in(0,T], \end{cases} \quad (22)$$

where

$$\begin{aligned} \ell_\in^M \Upsilon^{j+1}(x) &= -\left(\in + \tau_j a^{j+1}(x)\right)\left(w_{xx}(x)\right)^{j+1} \\ &\quad + d^{j+1}(x)\left(w_x(x)\right)^{j+1} \\ &\quad +\left(\in + \tau_j c^{j+1}(x)\right)w^{j+1}(x) \end{aligned}$$

and $g(x,t_{j+1}) = -\varepsilon\left(w_{xx}(x)\right)^j + \varepsilon w^j(x) + \tau_j \aleph^{j+1}(x)$.

Definition 3.1. [6, 12, 25, 27, 28] A FDM is stable for $\|.\|$, if there exists positive constants L1 and L2, independent from τ_j, such that when τ_j approaches τ_1 and τ_2, we have

$$\left\|w^j\right\| \le L_1\left\|w^0\right\| + L_2\left\|\aleph\right\|.$$

Here, w^0 represents the initial condition, while $\aleph$ denotes the source term.

Lemma 3.2. [22, 27, 28] Let the function $\Upsilon\in C^0\left(\overline{\Lambda}\right)\cap C^2(\Lambda)$. Then we have

$$\|\Upsilon\| \le \|\Upsilon\|_{\partial\Omega} + \left\|\ell_\varepsilon^M \Upsilon^{j+1}(x)\right\|_{\overline{\Lambda}}.$$

Lemma (3.2) ensures that Eq. (22) admits unique solution $\Upsilon^{j+1}(x)$ at time level τ_j. Moreover, by Lemma (3.2), this solution $\Upsilon^{j+1}(x)$ remains uniformly bounded with respect to ε. Define $\Xi^{j+1}(x) = \Upsilon(x,t_{j+1}) - \overline{\Upsilon}(x,t_{j+1})$, as the local error of Eq. (22) at t_{j+1}, where $\overline{\Upsilon}\left(x,t_{j+1}\right)$ solves the corresponding auxiliary BVP:

$$\begin{cases} \ell_{\varepsilon}^{M}\overline{\Upsilon}^{j+1}\left(x\right)=g\left(x,t_{j+1}\right), \\ \overline{\Upsilon}^{j+1}\left(0\right)=0=\overline{\Upsilon}^{j+1}\left(1\right),\ \ 0\le j\le M. \end{cases} \tag{23}$$

Lemma 3.3. (Local Truncation Error(LTE)): The local error $\Xi^{j+1}\left(x\right)$ obeys the following bound:

$$\left\|\Xi^{j+1}\left(x\right)\right\|\le C\left(\Delta t\right)^{2},\ \text{ where } \Delta t=M^{-1}\ln\left(M\right). \tag{24}$$

Proof. Depending on the magnitude of σ, there arise two conditions:

1. If $j=0(1)\dfrac{M}{2}$, $t_j=j\tau_1$ and $\tau_1=\dfrac{2\sigma}{M}$, then we have

$$\begin{aligned} \tau_j &= t_j-t_{j-1}=j\tau_1-\left(j-1\right)\tau_1 \Rightarrow \\ t_j &= \tau_1=\frac{2\alpha_0^{-1}\varepsilon\ln(M)}{M} \\ &\le KM^{-1}\ln(M), K=2\alpha_0^{-1}\varepsilon \end{aligned}$$

Evaluating at t_{j+1} with $\tau_j=\Delta t=KM^{-1}\ln(M)$ and applying Taylor expansion to Eqs. (19) and (22), we get

$$\begin{cases} \ell_{\varepsilon}^{M}\Xi^{j+1}(x)=K_1\left(M^{-1}\ln(M)\right)^{2},\ K_1=K^{2},\ x\in\Omega, \\ \Xi^{j+1}\left(0\right)=0=\Xi^{j+1}\left(l\right),\ \ j=0(1)M/2. \end{cases} \tag{25}$$

2. If $j=\dfrac{M}{2}+1,\ldots,M$, $t_j=\sigma+\left(j-\dfrac{M}{2}\right)\tau_2$ and $\tau_2=\dfrac{2\left(1-\sigma\right)}{M}$. Now

$$\begin{aligned} \tau_j=t_j-t_{j-1} &= \sigma+\left(j-M/2\right)\tau_2-\left(\sigma+\left(\left(j-1\right)-M/2\right)\tau_2\right), \\ &= \sigma+\left(j-M/2\right)\tau_2-\sigma-j\tau_2+\tau_2+M/2\tau_2, \\ &= \tau_2=2\frac{1-\alpha_0^{-1}\varepsilon\ln(M)}{M}, \\ &\le K_4M^{-1},\ \text{since } 2\alpha_0^{-1}\varepsilon\ln(M)\le 2M^{-1}. \end{aligned}$$

Considering the estimate at $t_{j+1}=\Delta t_2=K_4M^{-1}$ and applying Taylor series expansion to Eqs. (22) and (19), we get:

$$\begin{cases} \ell_{\varepsilon}^{N,M}\Xi^{j+1}\left(x\right)=K_5\left(M^{-1}\right)^{2},\ K_5=K_4^{2},\ x\in\Omega, \\ \Xi^{j+1}\left(0\right)=0=\Xi^{j+1}\left(l\right),\ j=(M/2)+1(1)M. \end{cases} \tag{26}$$

Applying Lemma (3.2) to $\Xi^{j+1}\left(x\right)$ yields estimates for both regions. The total LTE is expressed as the sum of the finer-and coarse-mesh contributions, i.e.,

$$\begin{aligned} \left\|\Xi^{j+1}\left(x\right)\right\| &= K_1\left(M^{-1}\ln(M)\right)^{2}+K_5\left(M^{-1}\right)^{2}, \\ &= C\left(M^{-1}\ln(M)\right)^{2},\ C=K_1+K_5\left(M^{-1}\right)^{2}. \end{aligned} \tag{27}$$

Lemma 3.4. (Global Error). The global error $\Sigma^{j}\left(x\right)$ is bounded at t_j as follows:

$$\sup_{(j+1)\Delta t\le T}\le K_*\left(\Delta t\right),\ \Delta t=M^{-1}\ln(M). \tag{28}$$

Proof. Let $\left\|\Sigma^{j}\left(x\right)\right\|=\Upsilon(x,t_{j+1})-\overline{\Upsilon}(x,t_{j+1})$. By applying Eq. (27) togher with Lemma (3.3), we obtain the global error at $(j+1)th$ time step.

$$\begin{aligned} \left\|\Sigma^{j}\left(x\right)\right\|_{\infty} &= \left|\sum_{l=1}^{j}\Xi_l\right|,\ j\le T/\Delta t,\ \Delta t=K\left(M^{-1}\ln(M)\right)^{2}, \\ &\le \left\|\Xi_1\right\|_{\infty}+\left\|\Xi_2\right\|_{\infty}+\ldots+\left\|\Xi_j\right\|_{\infty}, \\ &\le C_1 j\left(\Delta t\right)^{2},\ \ \text{using } Eq.(3.10) \\ &\le C_1\left(jM^{-1}\ln(M)\right)\left(M^{-1}\ln(M)\right), \\ &\le C_1T\left(M^{-1}\ln(M)\right),\ \text{as } j\left(M^{-1}\ln(M)\right)\le T, \\ &\le C_4\left(M^{-1}\ln(M)\right),\ \ C_4=C_3T. \end{aligned}$$

Spatial Semi-Discretization

The TCBS method is employed to approximate the solution of Eq. (21) and its spatial derivatives using linear spline expansions.

Cubic Trigonometric B-Spline Techniques

The domain Λ divided into N equal intervals, the approximate solution at $(j+1)th$ is expressed as:

$$W\left(x,t\right)=\sum_{i=-1}^{N+1}\delta_i\left(t\right)CTB_i\left(x\right), \tag{29}$$

where $\delta_i(t)$ are determined to approximate $W(x,t)$ to exact solution $W_e(x,t)$ at (x_i, t_j), and $CTB_i(x)$ represent the TCBS basis functions , which is given as[29-30]

$$CTB_i\left(x\right)=\frac{1}{\vartheta}\begin{cases} \sin^3\left(\xi_1\right), & \text{if } \left[x_{i-2},x_{i-1}\right] \\ \sin\left(\xi_1\right)\left[\sin\left(\xi_1\right)\sin\left(\xi_2\right)+\sin\left(\xi_3\right)\sin\left(\xi_4\right)\right] & \\ \quad +\sin^2\left(\xi_4\right)\sin\left(\xi_5\right), & \text{if } \left[x_{i-1},x_i\right], \\ \sin\left(\xi_5\right)\left[\sin\left(\xi_4\right)\sin\left(\xi_3\right)+\sin\left(\xi_5\right)\sin\left(\xi_6\right)\right] & \\ \quad +\sin\left(\xi_1\right)\sin^2\left(\xi_3\right), & \text{if } \left[x_i,x_{i+1}\right] \\ \sin^3\left(\xi_5\right), & \text{if } \left[x_{i+1},x_{i+2}\right] \\ 0, & \text{otherwise,} \end{cases} \tag{30}$$

where, $\vartheta=\sin\left(\xi\right)\sin\left(2\xi\right)\sin\left(3\xi\right)$, $\xi=\dfrac{h}{2}$, $\xi_1=\dfrac{x-x_{i-2}}{2}$, $\xi_2=\dfrac{x_i-x}{2}$, $\xi_3=\dfrac{x_{i+1}-x}{2}$, $\xi_4=\dfrac{x-x_{i-1}}{2}$, $\xi_5=\dfrac{x_{i+2}-x}{2}$ and $\xi_6=\dfrac{x-x_i}{2}$. Consider the iterative relation provided in Eq. (31).

Table 1. The values of $CTB_i(x)$, $CTB_i'(x)$ and $CTB_i''(x)$ at the nodal points obtained using Eq. (30)

	x_{i-2}	x_{i-1}	x_i	x_{i+1}	x_{i+2}
$CTB_i(x)$	0	μ_1	μ_2	μ_1	0
$CTB_i'(x)$	0	μ_3	0	μ_4	0
$CTB_i''(x)$	0	μ_5	μ_6	μ_5	0

$$CTB_i^k(x) = \frac{\sin\left(\frac{x-x_i}{2}\right)}{\sin\left(\frac{x_{i+k-1}-x_i}{2}\right)} CTB_i^{k-1}(x) + \frac{\sin\left(\frac{x_{i+k}-x}{2}\right)}{\sin\left(\frac{x_{i+k}-x_{i+1}}{2}\right)} CTB_i^{k-1}(x), \quad k = 2,\dots. \tag{31}$$

This iterative formula defines TCBS, beginning with first order case. Table 1 display $CTB_i(x)$ and its derivative values at the mesh points.

Table 1 lists the entries as:

$$\mu_1 = \sin^2(\zeta)\csc(2\zeta)\csc(3\zeta),\ \mu_2 = \frac{2}{1+2\cos(2\zeta)},$$
$$\mu_3 = -\frac{3}{4}\csc(3\zeta),\ \mu_4 = \frac{3}{4}\csc(3\zeta),$$
$$\mu_5 = \frac{3(1+3\cos(2\zeta))\csc^2(\zeta)}{16(2\cos(\zeta)+\cos)(3\zeta)},\ \mu_6 = \frac{-3\cot^2(3\zeta)}{2+4\cos(2\zeta)},$$
where $\zeta = \frac{h}{2}$.

The approximation W_i^j at (x_i, t_j) over sub-interval $[x_i, x_{i+1}]$ is given as:

$$W_i^j = \sum_{i=-1}^{N+1} \delta_i^{j+1} CTB_i(x). \tag{32}$$

Owing to the local support of B-splines, only $CTB_{i-1}(x)$, $CTB_i(x)$ and $CTB_{i+1}(x)$ are non-zero on the given interval. Using Eqs. (30) and (32), the nodal values and derivatives of W_i^j are expressed through the time parameters δ_i^{j+1} as follows:

$$\begin{cases} W_i^{j+1} = \mu_1\delta_{i-1}^{j+1} + \mu_2\delta_i^{j+1} + \mu_1\delta_{i+1}^{j+1}, \\ (W_x)_i^{j+1} = \mu_3\delta_{i-1}^{j+1} + \mu_4\delta_{i+1}^{j+1}, \\ (W_{xx})_i^{j+1} = \mu_5\delta_{i-1}^{j+1} + \mu_6\delta_i^{j+1} + \mu_5\delta_{i+1}^{j+1}. \end{cases} \tag{33}$$

The approximate solution at the mesh boundaries is obtained from Eq. (32) combined with the boundary conditions in (2.1) as follows:

$$\begin{cases} W(x_0, t_{j+1}) = \mu_1\delta_{-1}^{j+1} + \mu_2\delta_0^{j+1} + \mu_1\delta_1^{j+1} = 0, \\ W(x_N, t_{j+1}) = \mu_1\delta_{N-1}^{j+1} + \mu_2\delta_N^{j+1} + \mu_1\delta_{N+1}^{j+1} = 0. \end{cases} \tag{34}$$

Once δ_i is computed and $CTB_i(x)$ with its derivatives are substituted into Eq. (21), we obtain $N + 1$ equations with $N + 3$ unknowns.

$$\begin{aligned} \ell_\varepsilon^{N,M} W &= r_i^- \delta_{i-1}^{j+1} + r_i^c \delta_i^{j+1} + r_i^+ \delta_{i+1}^{j+1} \\ &= E_i^- \delta_{i-1}^j + E_i^c \delta_i^j + E_i^+ \delta_{i+1}^j + F_i, \\ &\text{for } i = 0,1,\dots,N, \end{aligned} \tag{35}$$

where, the coefficients take the following form

$$\begin{cases} r_i^- = \varepsilon(\mu_1 - \mu_5) - \tau_j\mu_5 a_i^{j+1} + \tau_j\mu_3 a_i^{j+1} + \tau_j\mu_1 c_i^{j+1}, \\ r_i^c = \varepsilon(\mu_2 - \mu_6) - \tau_j\mu_6 a_i^{j+1} + \tau_j\mu_2 c_i^{j+1}, \\ r_i^+ = \varepsilon(\mu_1 - \mu_5) - \tau_j\mu_5 a_i^{j+1} + \tau_j\mu_3 d_i^{j+1} + \tau_j\mu_1 c_i^{j+1}, \\ E_i^- = \varepsilon(\mu_1 - \mu_5),\ E_i^c = \varepsilon(\mu_2 - \mu_6), \\ E_i^+ = \varepsilon(\mu_1 - \mu_5),\ F_i = \tau_j \aleph_i^{j+1}. \end{cases} \tag{36}$$

Treatement of boundary conditions

To eliminate δ_{-1} and δ_{N+1} from Eq. (35), we apply boundary conditions given in Eq. (34). Now, for $i = 0$, Eq. (35) is reduced to

$$\left(r_0^c - r_0^- \frac{\mu_2}{\mu_1}\right)\delta_0^{j+1} + \left(r_0^+ - r_0^-\right)\delta_1^{j+1} = \left(E_0^c - E_0^- \frac{\mu_2}{\mu_1}\right)\delta_0^j + \left(E_0^+ - E_0^-\right)\delta_1^j + F_0. \tag{37}$$

Eq. (35) simplified to the form for $i = N$

$$\left(r_N^- - r_N^+\right)\delta_{N-1}^{j+1} + \left(r_N^c - r_N^+ \frac{\mu_2}{\mu_1}\right)\delta_N^{j+1} = \left(E_N^- - E_N^+\right)\delta_{N-1}^j + \left(E_N^c - E_N^+ \frac{\mu_2}{\mu_1}\right)\delta_N^j + F_N. \tag{38}$$

Now, Eqs. (35)- (38) lead to $(N + 3) \times (N + 3)$ system with $(N + 3)$ unkowns $\delta_{-1}, \delta_0, \dots, \delta_N, \delta_{N+1}$. Excluding the unkowns δ_{-1} and δ_{N+1} from Eq. (37) and Eq. (38) for $i = 0$ and $i = N$, then Eq. (35) becomes $(N + 1) \times (N + 1)$.

equations with $(N + 1)$ unknowns $\delta_0, ..., \delta_{N-1}, \delta_N$ in matrix form as

$$A\delta_i^{j+1} = B\delta_i^j + F, \quad i = 1,2,...,N-1. \tag{39}$$

The elements of the tridiagonal matrices $A = \omega_{ij}$ and $B = \psi_{ij}$ are defined as follows:

$$A = \begin{bmatrix} p_1 & p_2 & 0 & 0 & \dots & 0 & 0 & 0 \\ r_1^- & r_1^c & r_1^+ & 0 & \cdots & 0 & 0 & 0 \\ 0 & r_2^- & r_2^c & r_2^+ & \cdots & 0 & 0 & 0 \\ \vdots & \vdots & \vdots & \ddots & \ddots & \vdots & \vdots & \vdots \\ 0 & 0 & 0 & 0 & \cdots & r_{N-1}^- & r_N^c & r_{N+1}^+ \\ 0 & 0 & 0 & 0 & \cdots & 0 & p_3 & p_4 \end{bmatrix},$$

$$B = \begin{bmatrix} p_5 & p_6 & 0 & 0 & \dots & 0 & 0 & 0 \\ E_1^- & E_1^c & E_1^+ & 0 & \cdots & 0 & 0 & 0 \\ 0 & E_2^- & E_2^c & E_2^+ & \cdots & 0 & 0 & 0 \\ \vdots & \vdots & \vdots & \ddots & \ddots & \vdots & \vdots & \vdots \\ 0 & 0 & 0 & 0 & \cdots & E_{N-1}^- & E_N^c & E_{N+1}^+ \\ 0 & 0 & 0 & 0 & \cdots & 0 & p_7 & p_8 \end{bmatrix}.$$

The entries of the given matrix are

$$p_1 = \left(r_0^c - r_0^- \frac{\mu_2}{\mu_1}\right),\ p_2 = \left(r_0^+ - r_0^-\right),$$

$$p_3 = \left(r_N^- - r_N^+\right),\ p_4 = \left(r_N^c - r_N^+ \frac{\mu_2}{\mu_1}\right),$$

$$p_5 = \left(E_0^c - E_0^- \frac{\mu_2}{\mu_1}\right),\ p_6 = \left(E_0^+ - E_0^-\right),$$

$$p_7 = \left(E_N^- - E_N^+\right), p_8 = \left(E_N^c - E_N^+ \frac{\mu_2}{\mu_1}\right).$$

The vectors δ^{j+1} and F are defined as:

$$\delta_i^{j+1} = \left(\delta_{-1}^{j+1}, \delta_0^{j+1}, \delta_N^{j+1}, \delta_{N+1}^{j+1}\right)^T \text{ and } F = \tau_j\left(\aleph_0^{j+1}, \aleph_1^{j+1}, ..., \aleph_N^{j+1}, \aleph_{N+1}^{j+1}\right)^T.$$

Rearranging Eq. (39) gives

$$A\overline{X} = H, \text{ where } \overline{X} = \delta^{j+1}, \text{ and } H = B\delta_i^j + F. \tag{40}$$

The initial vector $\left(\delta_{-1}^0, ..., \delta_{N+1}^0\right)$ is determined by solving the corresponding interpolation for Eq. (35).

$$\begin{cases} \left(\dfrac{\partial W^0}{\partial x}\right)_0 = \left(\dfrac{\partial \varphi^0}{\partial x}\right)_0, & i = 0, \\ W^0(x_i) = \varphi^0(x_i), & i = 0(1)N, \\ \left(\dfrac{\partial W^0}{\partial x}\right)_l = \left(\dfrac{\partial \varphi^0}{\partial x}\right)_l, & i = N, \end{cases} \tag{41}$$

where $W^0(x) = \sum_{i=-1}^{N+1} \delta_i^0 CTB_i(x)$. Eq. (41), formulated for the initial conditions, consists of $N + 1$ equations and $N + 3$ unknowns. To solve the system, δ_{-1}^0 and δ_{N+1}^0 must be eliminated. After simplications, we obtain:

$$\begin{cases} \mu_2 \delta_0^0 + \left(\mu_1 - \dfrac{\mu_1\mu_4}{\mu_3}\right)\delta_1^0 = \varphi(0) - \dfrac{\mu_1}{\mu_3}\varphi'(0), \\ \mu_1 \delta_{i-1}^0 + \mu_2 \delta_i^0 + \mu_1 \delta_{i+1}^0 = \varphi(x_i), \quad i = 1(N-1), \\ \left(\mu_1 - \dfrac{\mu_1\mu_4}{\mu_3}\right)\delta_{N-1}^0 + \mu_2 \delta_N^0 = \varphi(x_N) - \dfrac{\mu_1}{\mu_3}\varphi'(x_N). \end{cases} \tag{42}$$

Now, Eq. (42) gives $(N + 1) \times (N + 1)$ system of equations. This system is easily solved for δ_0^0 using matrix inversion algorithm and provides the initial values for Eq. (39).

Stability Analysis

This section applies Von-Neumann stability analysis [8] to examine the scheme's stability. At knots with $\aleph(x,t) = 0$, substituting $W(x,t)$ and its derivatives into Eq. (35) yields the following difference equation in δ_i:

$$r_i^- \delta_{i-1}^{j+1} + r_i^c \delta_i^{j+1} + r_i^+ \delta_{i+1}^{j+1} = E_i^- \delta_{i-1}^j + E_i^c \delta_i^j + E_i^+ \delta_{i+1}^j, \tag{43}$$

where r_i^-, r_i^c, r_i^+ and E_i^-, E_i^c, E_i^+ are given in Eq. (36). Substituting trial solution

$$\delta_n^l = \zeta^l e^{in\eta h}, \tag{44}$$

where η is the wave number, l is the time level, ζ^l the Fourier coefficient, h the spatial step, $i = \sqrt{-1}$ the imaginary unit, and η the node index, into Eq. (43) gives:

$$\begin{aligned} &r_i^- \zeta^{l+1} e^{i(n-1)\eta h} + r_i^c \zeta^{l+1} e^{i(n)\eta h} + r_i^+ \zeta^{l+1} e^{i(n+1)\eta h} = \\ &E_i^- \zeta^l e^{i(n-1)\eta h} + E_i^c \zeta^l e^{in\eta h} + E_i^+ \zeta^l e^{i(n+1)\eta h}. \end{aligned} \tag{45}$$

Dividing Eq. (45) by $e^{in\varphi}$, where $\varphi = \eta h$ and rearranging to obtain

$$\frac{\zeta^{l+1}}{\zeta^l} = \Pi = \frac{E_i^c + E_i^- e^{-i\varphi} + E_i^+ e^{i\varphi}}{r_i^c + r_i^- e^{-i\varphi} + r_i^+ e^{i\varphi}}, \tag{46}$$

where Π is intensification factor. The error plenty should not intensify, so it is $|\Pi| \le 1$. Eq. (46) is reformulated by using Euler relation $e^{\pm i\varphi} = \cos(\varphi) \pm i\sin(\varphi)$,

$$\Pi = \frac{E_i^c + \left(E_i^- + E_i^+\right)\cos(\varphi) + i\left(E_i^+ + E_i^-\right)\sin(\varphi)}{r_i^c + \left(r_i^- + r_i^+\right)\cos(\varphi) + i\left(r_i^+ + r_i^-\right)\sin(\varphi)}. \tag{47}$$

From, Eq. (47), we obtain

$$\Pi = \frac{X_1 + iY_1}{X_2 + iY_2}. \tag{48}$$

By applying basic arithmetic manipulations to the complex numbers, Eq. (48) can be expressed in the following form:

$$\Pi = \frac{X_1X_2 + Y_1Y_2}{X_2^2 + Y_2^2} + i\frac{Y_1X_2 - X_1Y_2}{X_2^2 + Y_2^2}, \tag{49}$$

where

$$\begin{cases} X_1 = E_i^c + \left(E_i^- + E_i^+\right)\cos(\varphi), \; Y_1 = \left(E_i^+ + E_i^-\right)\sin(\varphi), \\ X_2 = r_i^c + \left(r_i^- + r_i^+\right)\cos(\varphi), \quad Y_2 = \left(r_i^+ + r_i^-\right)\sin(\varphi). \end{cases}$$

Since Π is a complex number, stability condition $|\Pi| \leq 1$ yields the relation

$$|\Pi| = \sqrt{\left(\frac{X_1X_2 + Y_1Y_2}{X_2^2 + Y_2^2}\right)^2 + \left(\frac{Y_1X_2 - X_1Y_2}{X_2^2 + Y_2^2}\right)^2} \leq 1. \tag{50}$$

By inserting $X_i, Y_i\ (i = 1,2)$ into Eq. (50) and since $\varphi = \eta h, 0 \leq \varphi \leq \pi$, the equation needs verification only at extreme values. Setting $\varphi = \pi$, gives:

$$\left(\frac{E_i^- - E_i^c + E_i^+}{r_i^- - r_i^c + r_i^+}\right)^2 \leq 1. \tag{51}$$

The inequality in Eq. (51) can be expressed equivalently as:

$$-1 \leq \frac{E_i^- - E_i^c + E_i^+}{r_i^- - r_i^c + r_i^+} \leq 1. \tag{52}$$

Substitution of these values of parameters r_i^-, r_i^c, r_i^+ and E_i^-, E_i^c, E_i^+ yields the relation

$$-1 \leq \frac{\varepsilon\left(2\mu_1 - \mu_2\right) + \varepsilon\left(\mu_6 - 2\mu_5\right)}{\Xi_1\left(2\mu_1 - \mu_2\right) + \Xi_2\left(\mu_6 - 2\mu_5\right) + \Xi_3} \leq 1 \Rightarrow |\Pi| \leq 1, \tag{53}$$

where $\Xi_1 = \varepsilon + \tau_j c_i^{j+1}$, $\Xi_2 = \varepsilon + \tau_j a_i^{j+1}$ and $\Xi_3 = 2\mu_3\tau_j d_i^{j+1}$. The inequalities in Eq. (53) hold universally, guaranteeing a non-vanishing denominator. Since the eigenvalue modulus does not exceed unity, the scheme with $\aleph(x,t) = 0$ is unconditionally stable, as shown in Eq. (4.12). This stability extends to the general case $\aleph(x,t)$ by Duhamel's principle [25], which asserts that stability for $P_{k,h}V = \aleph$ follows from stability for $P_{k,h}V = 0$. Consequently, no constraints are imposed on the spatial grid or temporal step size, though their selection should enhance the scheme's accuracy [8].

Analysis of Convergence

Lemma 5.1. [8, 30] The TCBS: $CTB_{-1},\ldots,CTB_{N+1}$ given in Eq. (32) gratify the inequality:

$$\sum_{i=-1}^{N+1}\left|CTB_i\left(x\right)\right| \leq 6, \; 0 \leq x \leq 1. \tag{50}$$

Proof. As $\left|\sum_{i=-1}^{N+1} CTB_i\left(x\right)\right| \leq \sum_{i=-1}^{N+1}\left|CTB_i\left(x\right)\right|$, at $x = x_i$, right side of Eq. (50)

$$\begin{aligned}\sum_{i=-1}^{N+1}\left|CTB_i\left(x\right)\right| &= \left|CTB_{i-2}\left(x\right)\right| + \left|CTB_{i-1}\left(x\right)\right| \\ &\quad + \left|CTB_i\left(x\right)\right| + \left|CTB_{i+1}\left(x\right)\right|, \\ &= \left|\mu_2\right| + \left|\mu_1\right| + \left|\mu_1\right| + \left|\mu_2\right| \leq 6.\end{aligned}$$

Thus, for all $x \in [0,1]$, we have

$$\begin{aligned}\sum_{i=-1}^{N+1}\left|CTB_i\left(x\right)\right| &= \left|CTB_{i-1}\left(x\right)\right| + \left|CTB_i\left(x\right)\right| \\ &\quad + \left|CTB_{i+1}\left(x\right)\right| \leq 6.\end{aligned}$$

Lemma 5.2. The approximation $CTB(x)$ from Eq. (32) is uniformly bounded, that is $\left|CTB(x)\right| \leq C,\ \forall x \in \overline{\Omega}$.

Proof. For the proof, we refer the reader to [8, 26, 29].

Let $\overline{w}(x)$, be the exact solution of BVPs Eq. (35)-(38), and also $W(x) = \sum_{i=-1}^{N+1}\delta_i CTB_i\left(x\right)$ be the TCBS approximation to the exact solution. Due to the round of errors[24, 29], let $\overline{W}(x) = \sum_{i=-1}^{N+1}\overline{\delta}_i CTB_i\left(x\right)$ is the computed CTBS approximation to $\overline{w}(x)$, where $\overline{\delta}_i = \left(\overline{\delta}_0, \overline{\delta}_1, \ldots, \overline{\delta}_N\right)^T$. To estimate , we must estimate the errors $\|\overline{w}(x) - \overline{W}(x)\|$ and $\|\overline{W}(x) - W(x)\|$ respectively. Following Eq. (40) for $\overline{W}(x)$, we obtain

$$A\overline{\overline{X}} = \overline{H}, \tag{51}$$

where $\overline{\overline{X}} = \left(\overline{\delta}_0, \overline{\delta}_1, \ldots, \overline{\delta}_N\right)^T$. Eqs. (40) and (51) together lead to:

$$A\left(\overline{X} - \overline{\overline{X}}\right) = H - \overline{H}. \tag{52}$$

Prior to continuing, the subsequent theorem is required:

Theorem 5.3. Suppose that $\Gamma\left(x\right) \in C^4\left[0,l\right]$ and $\left\{0 = x_0, \ldots, x_N = 1\right\}$ be partition of [0,l]. If $R(x)$ be the unique TCBS approximation for $\Gamma\left(x\right)$ at the knots $x_0, \ldots, x_{N-1}, x_N$, then

$$\begin{aligned}&\left\|R(x) - \Gamma\left(x\right)\right\| \leq O(h^3), \\ &\left\|R^{(k)}(x) - \Gamma^{(k)}\left(x\right)\right\| \leq O(h^2), \quad k = 1,2, \\ &\left\|R^{(k)}(x) - \Gamma^{(k)}\left(x\right)\right\| \leq O(h), \quad k = 3.\end{aligned}$$

Proof. Refer to [8, 25, 29] and the references cited therein.

Referring to Eq. (21) and Theorem 5.3, we obtain the bound on $\left\|H - \overline{H}\right\|$ as follows:

$$\left|H-\overline{H}\right| = \left|\alpha_1 u_j^{"} - \beta_1 u_j^{'} - \gamma_1 u_j - \alpha_1\left(\overline{u}\right)_j^{"} - \beta_1\left(\overline{u}\right)_j^{'} - \gamma_1 \overline{u}_j\right|,$$
$$\le \left|\alpha_1\right|\left|u_j^{"} - \left(\overline{u}\right)_j^{"}\right| + \left|\beta_1\right|\left|u_j^{'} - \left(\overline{u}\right)_j^{'}\right| + \left|\gamma_1\right|\left|u_j - \overline{u}_j\right|,$$

where $\alpha_1 = -\left(\varepsilon + \tau_j a_i^{j+1}\right)$, $\beta_2 = d_i^{j+1}$ and $\gamma_1 = \left(\varepsilon + \tau_j c_i^{j+1}\right)$. Then using Theorem 5.3,

$$\left\|H-\overline{H}\right\| \le \left|\alpha_1\right| O\left(h^2\right) + \left|\beta_1\right| O\left(h^2\right) + \left|\gamma_1\right| O\left(h^3\right),$$
$$\le \Theta h^2, \quad \text{where } \Theta = \left|\alpha_1\right| + \left|\beta_1\right| + \left|\gamma_1\right| O\left(h\right). \tag{53}$$

Substituting Eq. (53) into Eq. (52) yields

$$A\left(\overline{X}-\overline{\overline{X}}\right) = H - \overline{H} \Rightarrow \left\|\overline{X}-\overline{\overline{X}}\right\| \le \left\|A^{-1}\right\|\left\|H-\overline{H}\right\| \le \Theta h^2 \left\|A^{-1}\right\|. \tag{54}$$

Based on the given properties, TCBS basis functions vanish outside the interval $[x_{i-2}, x_{i+2}]$ while within this range, $CTB_i(x)$ assumes non-zero values at the mesh points. Likewise, their first and second derivatives exhibit similar behavior at these points. Consequently, the resulting matrix ||A|| takes the form of a tridiagonal band matrix characterized by dominant principal diagonal elements and non-zero off-diagonal entries. Therefore, A^{-1} remains bounded, and the matrix A is non-singular. Hence, we get:

$$\left\|\overline{X}-\overline{\overline{X}}\right\| \le \Theta_1 h^2, \quad \text{where } \Theta_1 = \Theta\left\|A^{-1}\right\|. \tag{55}$$

From $W(x) - \overline{W} = \sum_{i=-1}^{N+1}\left(\delta_i - \overline{\delta}_i\right) CTB_i\left(x\right)$, and Lemma (50), we get

$$\left\|\overline{W}\left(x\right) - W\left(x\right)\right\| \le \overline{\Theta} h^2, \text{ where } \overline{\Theta} = 6\Theta_1. \tag{56}$$

Theorem 5.4. Let $\overline{w}(x)$ be the exact solution of Eqs. (35)-(38) and let $W(x)$ be the TCBS collocation approximation, then

$$\left\|\overline{w}\left(x\right) - W\left(x\right)\right\| = O\left(h^2\right).$$

Proof. From Theorem 5.3, Eq. (56) and triangle inequalities, we have

$$\left\|\overline{w}\left(x\right) - W\left(x\right)\right\| = \left\|\overline{w}\left(x\right) - \overline{W}\left(x\right) + \overline{W}\left(x\right) - W(x)\right\|,$$
$$\le \left\|\overline{w}\left(x\right) - \overline{W}\left(x\right)\right\| + \left\|\overline{W}\left(x\right) - W\left(x\right)\right\|, \tag{57}$$
$$\le O\left(h^3\right) + \overline{\Theta}\left(h^2\right) \le O\left(h^2\right).$$

The convergent theorem below follows directly from Lemma (3.3-3.4) and Theorem 5.4.

Theorem 5.5. Let $\overline{w}(x)$ denote the exact solution to Eq. (1) and $W(x,t)$ its numerical approximation. Then, it follows that:

$$\left\|\overline{w}\left(x\right)\left(x_i, t_{j+1}\right) - W\left(x_i, t_{j+1}\right)\right\| \le C\left(M^{-1}\ln\left(M\right) + N^{-2}\right), \quad 0 \le i \le N, 0 \le j \le M. \tag{58}$$

RESULTS AND DISCUSSION

A representative numerical example is provided to illustrate the accuracy and performance of the proposed method. The absolute errors are computed using the double-mesh approach, and the maximum pointwise error corresponding to each value of ε is obtained through:

$$E_\varepsilon^{N,M} = \max_{0 \le i, j \le N, M}\left|W^{N,M}\left(x_i, t_j\right) - W^{2N,2M}\left(x_{2i}, t_{2j}\right)\right|, \tag{59}$$

where $W^{N,M}\left(x_i, t_j\right)$ is numerical solution at N, M mesh points whereas $W^{2N,2M}\left(x_{2i}, t_{2j}\right)$ denote the numerical solution at $2N$, $2M$ mesh points.

Example 6.1. Let us analyze the following illustrative problem from [16]:

$$\begin{cases} -\varepsilon \dfrac{\partial^3 w}{\partial t \partial x^2} + \varepsilon \dfrac{\partial w}{\partial t} - \dfrac{\partial}{\partial x}\left(\left(e^{-t} + \dfrac{1}{2}x^2 + 4\right)\dfrac{\partial w}{\partial x}\right) + \left(x^3 - t^2\right)\dfrac{\partial w}{\partial x} + \\ \qquad \left(e^{-t} + x^2\right)u = e^{-t}\sin\left(\pi x\left(1-x\right)\right), \\ w\left(x,0\right) = \sin\left(\pi x\right),\ x \in \overline{\Omega}_x, \\ w\left(0,t\right) = w(1,t) = 0,\ t \in (0,1]. \end{cases}$$

We can write Example (6.1) as, $d(x,t) = b(x,t) - \dfrac{\partial a}{\partial x} = \left(x^3 - x - t^2\right).$

$$\begin{cases} \varepsilon \dfrac{\partial w}{\partial t} - \varepsilon \dfrac{\partial^3 w}{\partial t \partial x^2} - \left(e^{-t} + \dfrac{1}{2}x^2 + 4\right)\dfrac{\partial^2 w}{\partial x^2} \\ + \left(x^3 - x - t^2\right)\dfrac{\partial w}{\partial x} + \left(e^{-t} + x^2\right)w \\ = e^{-t}\sin\left(\pi x\left(1-x\right)\right), \\ w\left(x,0\right) = \sin\left(\pi x\right),\ x \in \overline{\Omega}_x, \\ w\left(0,t\right) = w(1,t) = 0,\ t \in (0,1]. \end{cases}$$

The parameter $\alpha_0 = 1.999$ in Eq. (29) is chosen based on the boundedness of the solution, Lemma 2.2, and Definition 3.1.

The results are displayed through Tables and Figures. Tables (2), (3), and (4) list the computed maximum pointwise errors. Analysis of these tables demonstrates that the proposed method attains ε^- uniform convergence, with the maximum pointwise error consistently decreasing as the mesh sizes (N, M) increase for each value of ε.

Table 2. Maximum pointwise errors at discrete points with $N = M$ for various ε.

ϵ	$N = M = 8$	$N = M = 16$	$N = M = 32$	$N = M = 64$	$N = M = 12$	$N = M = 256$
10^{-2}	4.679e – 04	1.183e – 04	3.460e – 05	8.025e – 06	1.825 – 06	6.488 – 07
10^{-4}	4.658e – 04	1.186e – 04	3.586e – 05	7.718e – 06	1.840 – 06	7.559 – 07
10^{-6}	4.658e – 04	1.186e – 04	3.587e – 05	7.715e – 06	1.840 – 06	7.577 – 07
10^{-8}	4.658e – 04	1.186e – 04	3.587e – 05	7.715e – 06	1.840 – 06	7.578 – 07
10^{-10}	4.658e – 04	1.186e – 04	3.587e – 05	7.715e – 06	1.840 – 06	7.578 – 07
	⋮	⋮	⋮	⋮	⋮	⋮
10^{-20}	**4.658e – 04**	**1.186e – 04**	**3.587e – 05**	**7.715e – 06**	**1.840 – 06**	**7.578 – 07**
10^{-22}	**4.658e – 04**	**1.186e – 04**	**3.587e – 05**	**7.715e – 06**	**1.840 – 06**	**7.578 – 07**
$E_\varepsilon^{N,M}$	**4.679e – 04**	**1.186e – 04**	**3.587e – 05**	**8.025e – 06**	**1.840 – 06**	**7.578 – 07**

Table 3. Pointwise maximum errors for different values of ε, N and M.

ϵ ↓	$N = 16$ $M = 8$	$N = 32$ $M = 16$	$N = 64$ $M = 32$	$N = 128$ $M = 64$	$N = 256$ $M = 128$
10^{-2}	1.184e – 04	3.519e – 05	7.867e – 06	1.832e – 06	6.488e – 07
10^{-4}	1.186e – 04	3.586e – 05	7.716e – 06	1.840e – 06	7.559e – 07
10^{-6}	1.186e – 04	3.587e – 05	7.715e – 06	1.840e – 06	7.577e – 07
10^{-8}	1.186e – 04	3.587e – 05	7.715e – 06	1.840e – 06	7.578e – 07
10^{-10}	1.186e – 04	3.587e – 05	7.715e – 06	1.840e – 06	7.578e – 07
	⋮	⋮	⋮	⋮	⋮
10^{-20}	1.186e – 04	3.587e – 05	7.715e – 06	1.840e – 06	7.578e – 07
10^{-22}	1.186e – 04	3.587e – 05	7.715e – 06	1.840e – 06	7.578e – 07
$E_\varepsilon^{N,M}$	1.186e – 04	3.587e – 05	7.867e – 06	1.840e – 06	7.578e – 07

Table 4. Calculated $E_\varepsilon^{N,M}$ for a range of ε values and varying N and M.

ϵ ↓	$M = 10$ $N = 16$	$M = 20$ $N = 32$	$M = 40$ $N = 64$	$M = 80$ $N = 128$	$M = 160$ $N = 256$
10^{-2}	3.014e – 04	7.647e – 05	1.875e – 05	5.154e – 06	1.345e – 07
10^{-4}	3.031e – 04	7.742e – 05	1.894e – 05	5.607e – 06	1.216e – 07
10^{-6}	3.031e – 04	7.743e – 05	1.895e – 05	5.615e – 06	1.215e – 07
10^{-8}	3.031e – 04	7.743e – 05	1.895e – 05	5.615e – 06	1.215e – 07
10^{-10}	3.031e – 04	7.743e – 05	1.895e – 05	5.615e – 06	1.215e – 07
	⋮	⋮	⋮	⋮	⋮
10^{-20}	3.031e – 04	7.743e – 05	1.895e – 05	5.615e – 06	1.215e – 07
10^{-22}	3.031e – 04	7.743e – 05	1.895e – 05	5.615e – 06	1.215e – 07
$E_\varepsilon^{N,M}$	3.031e – 04	7.743e – 05	1.895e – 05	5.615e – 06	1345e – 07

Figure 1 shows the numerical solution profile for $N = M = 128$ and $\varepsilon = 10^{-2}$ highlighting the presence of an initial layer near $t = 0$. Figure 2 illustrates the solution for $N = M = 128$ and $\varepsilon = 10^{-8}$, clearly demonstrating that as $\varepsilon \to 0$, the solution develops steep gradients, with the surface plot becoming increasingly dense around the boundary layer region.

where the boundary layer forms. This dense clustering of the solution profile reflects the strong influence of the perturbation parameter and highlights the effectiveness of the numerical scheme in capturing the layer behaviour. Figure 3 displays the numerical solution profile obtained with $N = M = 256$, $\varepsilon = 10^{-8}$ using mesh plot. The figure reveals the

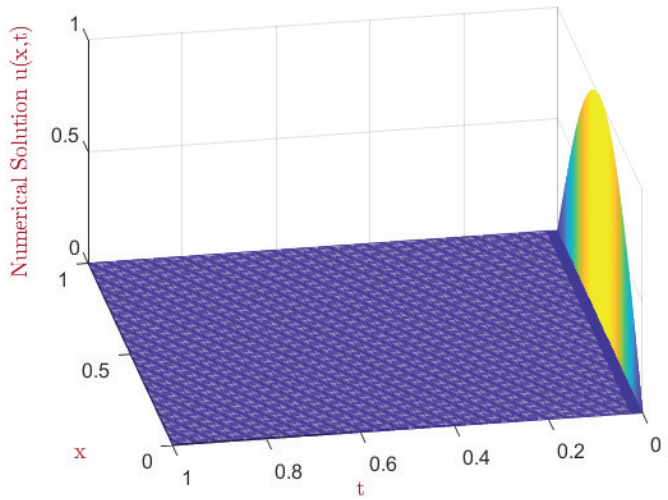

Figure 1. Mesh plot of the numerical solution profiles for $N = M = 128$, $\varepsilon = 10^{-2}$.

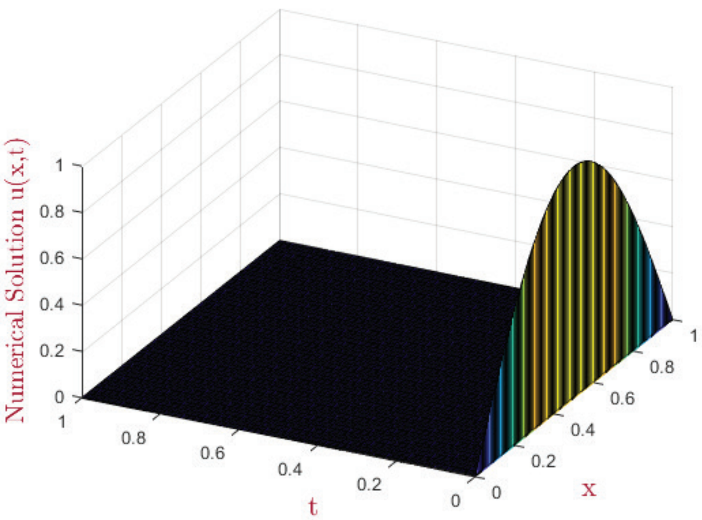

Figure 2. Surface plot illustrating the numerical solution for $N = M = 128$, $\varepsilon = 10^{-8}$.

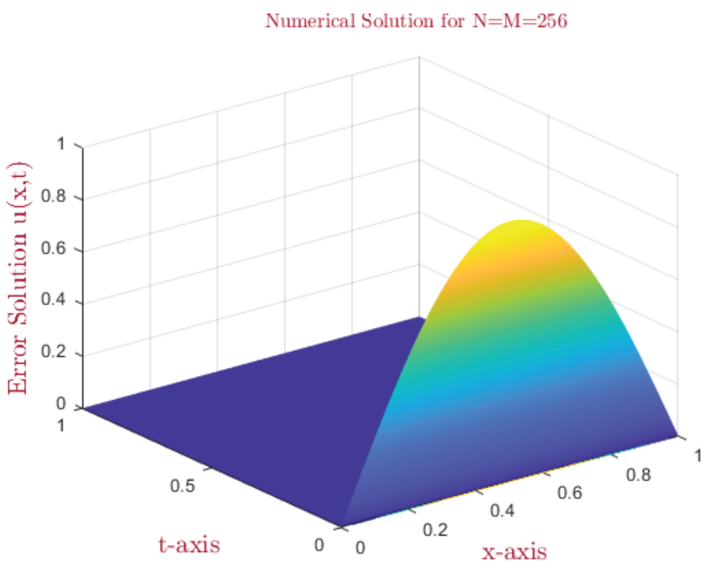

Figure 3. Numerical solution profiles corresponding to $N = M = 256$, $\varepsilon = 10^{-8}$.

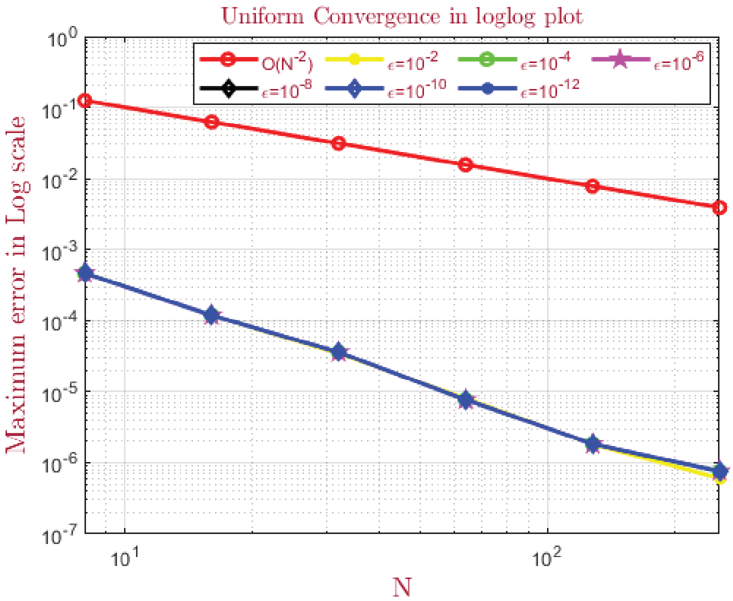

Figure 4. Log-log representation of the maximum point-wise error corresponding to Table 2.

presence of a pronounced intitial layer concentrated near $t = 0$, demonstrating the steep variation of the solution in the nearly region. In Figure 3, the log-log plot appears as a straight line, demonstrating the relationship between the numerical solution and the spatial variable. This linearity on the logarithmic scale indicates that although the error remains constant, the solution exhibits a power-law dependence on the spatial variable.

CONCLUSION

This study examines a numerical scheme designed for a class of SPSPs of one-dimensional IBVPs involving an initial jump. To obtain solutions that remain stable regardless of the perturbation parameter, a specialized difference scheme is introduced. The spatial derivatives are approximated using a uniform mesh combined with a TCBS based non-polynomial basis, while the temporal derivatives are treated with an Implicit Euler method on a Shishkin mesh. This combined approach effectively addresses the difficulties caused by the small perturbation parameter, particularly the formation of initial boundary layers. Compared to other cubic splines, the TCBS approach yields more accurate results. It encourages us to select this approach for the issue under consideration. From the analysis, it is demonstrated that the current scheme is convergent, independent of the perturbation parameter and mesh parameters. We look at a model example, and the computed results show that the proposed numerical method produces more accurate solutions for different values of ε, N and M. Our goal is to expand the current approach to include higher order SPSPs in upcoming work.

ACKNOWLEDGEMENT

The authors sincerely thank the anonymous reviewers for their insightful feedback, which greatly improved this manuscript. This work received no external funding or financial support.

AUTHORSHIP CONTRIBUTIONS

Authors equally contributed to this work.

DATA AVAILABILITY STATEMENT

The authors confirm that the data that supports the findings of this study are available within the article. Raw data that support the finding of this study are available from the corresponding author, upon reasonable request.

CONFLICT OF INTEREST

The author declared no potential conflicts of interest with respect to the research, authorship, and/or publication of this article.

ETHICS

There are no ethical issues with the publication of this manuscript.

STATEMENT ON THE USE OF ARTIFICIAL INTELLIGENCE

Artificial intelligence was not used in the preparation of the article.

REFERENCES

[1] Khompysh K, Shakir AG. An inverse source problem for a nonlinear pseudoparabolic equation with p-Laplacian diffusion and damping term. Quaest Math 2023;46:1889–1914. [CrossRef]

[2] Amiraliyev GM, Mamedov YD. Difference schemes on the uniform mesh for singularly perturbed pseudo-parabolic equations. Turk J Math 1995;19:207–222.

[3] Chiyaneh AB, Duru H. On adaptive mesh for the initial boundary value singularly perturbed delay Sobolev problems. Numer Methods Partial Differ Equ 2020;36:228–248. [CrossRef]

[4] Chiyaneh AB, Durus H. Uniform difference method for singularly pertubated delay Sobolev problems. Quaest Math 2020;43:1713–1736. [CrossRef]

[5] Duru H. Difference schemes for the singularly perturbed Sobolev periodic boundary problem. Appl Math Comput 2004;149:187–201. [CrossRef]

[6] Sobolev SL. Selected works of SL Sobolev. Volume I: Equations of Mathematical Physics, Computational Mathematics, and Cubature Formulas. London, Berlin, New York: Springer Nature; 2006.

[7] Mohapatra J, Shakti D. Numerical treatment for the solution of singularly perturbed pseudo-parabolic problem on an equidistributed grid. Nonlinear Eng 2020;9:169–174. [CrossRef]

[8] Zahra W. Trigonometric B-spline collocation method for solving PHI-four and Allen–Cahn equations. Mediterr J Math 2017;14:122. [CrossRef]

[9] Ewing RE. Numerical solution of Sobolev partial differential equations. SIAM J Numer Anal 1975;12:345–363. [CrossRef]

[10] Gu H. Characteristic finite element methods for nonlinear Sobolev equations. Appl Math Comput 1999;102:51–62. [CrossRef]

[11] Amiraliyev GM, Amiraliyeva IG. Difference schemes for the singularly perturbed Sobolev equations. In: Proc Int Conf Differ Equ Spec Funct Appl 2007. p. 23–40. [CrossRef]

[12] Amirali I. Analysis of higher order difference method for a pseudo-parabolic equation with delay. Miskolc Math Notes 2019;20:755–766. [CrossRef]

[13] Amirali I, Amiraliyev GM. Three layer difference method for linear pseudo-parabolic equation with delay. J Comput Appl Math 2022;401:113786. [CrossRef]

[14] Amiraliyev GM, Cimen E, Amirali I, Cakir M. High-order finite difference technique for delay pseudo-parabolic equations. J Comput Appl Math 2017;321:1–7. [CrossRef]

[15] Zhang C, Tan Z. Linearized compact difference methods combined with Richardson extrapolation for nonlinear delay Sobolev equations. Commun Nonlinear Sci Numer Simul 2020;91:105461. [CrossRef]

[16] Amiraliyev GM, Duru H, Amiraliyeva IG. A parameter-uniform numerical method for a Sobolev problem with initial layer. Numer Algorithms 2007;44:185–203. [CrossRef]

[17] Gunes B, Duru H. A second-order difference scheme for the singularly perturbed Sobolev problems with third type boundary conditions on Bakhvalov mesh. J Differ Equ Appl 2022;28:385–405. [CrossRef]

[18] Gunes B, Duru H. A computational method for the singularly perturbed delay pseudo-parabolic differential equations on adaptive mesh. Int J Comput Math 2023;100:1667–1682. [CrossRef]

[19] Cheru SL, Duressa GF, Mekonnen TB. Adaptive mesh extended cubic B-spline method for singularly perturbed delay Sobolev problems. Tamkang J Math 2025;56:165–185. [CrossRef]

[20] Clavero C, Jorge JC, Lisbona F. Uniformly convergent schemes for singular perturbation problems combining alternating directions and exponential fitting techniques. Appl Adv Comput Methods Bound Inter Layers 1993:33–52.

[21] Daba IT, Duressa GF. Extended cubic B-spline collocation method for singularly perturbed parabolic differential-difference equation arising in computational neuroscience. Int J Numer Methods Biomed Eng 2021;37:e3418. [CrossRef]

[22] Gelu FW, Duressa GF. A uniformly convergent collocation method for singularly perturbed delay parabolic reaction-diffusion problem. Abstr Appl Anal 2021;2021:8835595. [CrossRef]

[23] Cheru SL, Duressa GF, Mekonnen TB. Robust numerical approach for singularly perturbed parabolic problems with discontinuous convection coefficients and source terms. Comput Methods Differ Equ 2025;30:e03064. [CrossRef]

[24] Hall CA. On error bounds for spline interpolation. J Approx Theory 1968;1:209–218. [CrossRef]

[25] Nikolis A, Seimenis I. Solving dynamical systems with cubic trigonometric splines. Appl Math E-Notes 2005;5:116–123.

[26] Strikwerda JC. Finite difference schemes and partial differential equations. Philadelphia: Soc Ind Appl Math; 2004. [CrossRef]

[27] Gao F, Cui J, Zhao G. Weak Galerkin finite element methods for Sobolev equation. J Comput Appl Math 2017;317:188–202. [CrossRef]

[28] Nikan O, Avazzadeh Z. A localisation technique based on radial basis function partition of unity for solving Sobolev equation arising in fluid dynamics. Appl Math Comput 2021;401:126063. [CrossRef]

[29] Rektorys K. Variational methods in mathematics, science and engineering. Dordrecht: Springer Sci Bus Media; 2012.

[30] Singh S, Kumar D, Deswal K. Trigonometric B-spline based ε-uniform scheme for singularly perturbed problems with Robin boundary conditions. J Differ Equ Appl 2022;28:924–945. [CrossRef]